



RESEARCH ARTICLE

Track density imaging in progressive supranuclear palsy: A pilot study

Salvatore Nigro¹  | Maria Giovanna Bianco² | Gennarina Arabia³ | Maurizio Morelli³ | Rita Nisticò⁴ | Fabiana Novellino⁴ | Maria Salsone⁴ | Antonio Augimeri⁵ | Aldo Quattrone^{3,4,6} 

¹Department of Experimental and Clinical Medicine, Magna Graecia University, Catanzaro, Italy

²Department of Health Sciences, Magna Graecia University, Catanzaro, Italy

³Department of Medical and Surgical Sciences, Institute of Neurology, Magna Graecia University, Catanzaro, Italy

⁴Institute of Bioimaging and Molecular Physiology, National Research Council, Catanzaro, Italy

⁵Biotecnomed S.C.a.R.L, Catanzaro, Italy

⁶Neuroscience Center, Magna Graecia University, Catanzaro, Italy

Correspondence

Aldo Quattrone, Institute of Neurology, Department of Medical and Surgical Sciences, University Magna Graecia, 88100, Catanzaro, Italy.
Email: aldo.quattrone@gmail.com

Abstract

Progressive supranuclear palsy (PSP) is a neurodegenerative disorder characterized by white matter (WM) changes in different supra- and infratentorial brain structures. We used track density imaging (TDI) to characterize WM microstructural alterations in patients with PSP-Richardson's Syndrome (PSP-RS). Moreover, we investigated the diagnostic utility of TDI in distinguishing patients with PSP-RS from those with Parkinson's disease and healthy controls (HC). Twenty PSP-RS patients, 21 PD patients, and 23 HC underwent a 3 T MRI diffusion-weighted (DW) imaging. Then, we combined constrained spherical deconvolution and WM probabilistic tractography to reconstruct track density maps by calculating the number of WM streamlines traversing each voxel. Voxel-wise analysis was performed to assess group differences in track density maps. A support vector machine (SVM) approach was also used to evaluate the performance of TDI for discriminating between groups. Relative to PD patients, decreases in track density in PSP-RS patients were found in brainstem, cerebellum, thalamus, corpus callosum, and corticospinal tract. Similar findings were obtained between PSP-RS patients and HC. No differences in TDI were observed between PD and HC. SVM approach based on whole-brain analysis differentiated PD patients from PSP-RS with an area under the curve (AUC) of 0.82. The AUC reached a value of 0.98 considering only the voxels belonging to the superior cerebellar peduncle. This study shows that TDI may represent a useful approach for characterizing WM alterations in PSP-RS patients. Moreover, track density decrease in PSP could be considered a new feature for the differentiation of patients with PSP-RS from those with PD.

KEYWORDS

progressive supranuclear palsy, superior cerebellar peduncle, support vector machine, track density imaging, white matter

1 | INTRODUCTION

Progressive supranuclear palsy (PSP) is a rare neurodegenerative disorder characterized by abnormal tau pathology in the form of globose neurofibrillary tangles, tufted astrocytes, coiled bodies, and threads, with a predominance of 4-repeat (4R) tau isoforms (Dickson, Hauw, Agid, & Litvan, 2011; Hauw et al., 1994; Whitwell et al., 2017). Richardson's syndrome (PSP-RS) is the most common clinical variant of PSP with an early onset of a symmetric akinetic-rigid syndrome

with vertical supranuclear gaze palsy, early backward falls and frontal dysfunction (Litvan et al., 1996; Williams et al., 2005). Clinical diagnosis of PSP is often difficult, especially in the early stages of disease, when its symptoms and signs overlap with those of Parkinson's disease (PD) (Hughes, Daniel, Ben-Shlomo, & Lees, 2002; Osaki et al., 2004). However, the correct diagnosis of PSP is important for earlier suitable patient management, prognosis, and selection of the most appropriate treatments. Moreover, early differentiation between PSP and PD may provide a better patients selection in clinical trials.

Over the past two decades, several neuroimaging biomarkers have been described as potentially helpful in differentiating PSP from other parkinsonian syndromes (Whitwell et al., 2017). In particular, white matter (WM) degeneration evaluated using diffusion tensor imaging (DTI) has been demonstrated to be a striking feature of PSP-RS (Canu et al., 2011; Cochrane & Ebmeier, 2013; Nicoletti et al., 2006, 2008, 2013; Ohshita et al., 2000; Prodoehl et al., 2013; Saini et al., 2012; Seppi et al., 2003; Tessitore et al., 2014; Tsukamoto et al., 2012; Whitwell, Master, et al., 2011). DTI is a valuable noninvasive imaging technique for the assessment of the WM structure of the brain. WM integrity is often assessed locally using diffusion tensor derived metrics such as mean diffusivity (MD), which measures the magnitude of diffusion, or fractional anisotropy (FA), which quantifies the preferential direction of water diffusion along white matter tracts (Pierpaoli & Basser, 1996; Wieshmann et al., 1999). In patients with PSP-RS, relative to PD patients and healthy controls, a greater WM degeneration (lower FA and higher MD) have been observed in the superior cerebellar peduncles, cerebellum, corpus callosum, cingulum, superior longitudinal fasciculus, and white matter laminar of thalamus (Blain et al., 2006; Canu et al., 2011; Erbetta et al., 2009; Ito, Makino, Shirai, & Hattori, 2008; Knake et al., 2010; Piattella et al., 2015; Saini et al., 2012; Surova et al., 2015). Longitudinal studies found also that WM tract changes in patients with PSP-RS correlated with the progression of disease severity, behavioral dysfunction, and ocular motor decline (Agosta et al., 2018).

In recent years, several studies used DTI and fiber-tracking algorithm to reconstruct whole brain WM pathways and then to extract more detailed information about WM tract properties. In this regard, track-weighted (TW) imaging has been proposed as a robust and innovative approach able to provide a spatial resolution beyond the acquired data (super-resolution) and a novel anatomical contrast that cannot be obtained with conventional MRI (Calamante, Tournier, Jackson, & Connelly, 2010; Calamante et al., 2012; Calamante, 2017). In this approach, a TW image can be generated using information of streamline themselves, such as the number of streamlines in each voxel (i.e., track density imaging, TDI) (Calamante et al., 2010) or their average length (Pannek et al., 2011). TW imaging has recently been used in several studies revealing optimal performance in characterize brain anatomical features both in healthy controls and in several pathological conditions (Attyé et al., 2018; Bozzali et al., 2011; Pannek et al., 2011; Ziegler et al., 2014). For example, a recent study using TW imaging found significant alterations in track density of brainstem and nigrostriatal pathways in PD patients, relative to controls (Ziegler et al., 2014).

In this study, we used the track density imaging to characterize the WM microstructural alterations in patients with PSP-RS patients compared with those with PD and healthy controls. Considering the diffusion properties alterations observed in WM tracts of PSP-RS patients together with damages reported in pathological studies, we hypothesized that patients with PSP-RS would exhibit an extensive decrease in fibers density in several WM pathways including brainstem, superior cerebellar peduncles, superior longitudinal fasciculus and corpus callosum. Moreover, we assessed whether these fibers density alterations could differentiate patients with PSP-RS from those with PD and healthy controls at an individual level. To this end,

we investigated the diagnostic accuracy of an image-based classification between PSP-RS and PD in individual patients by using TDI.

2 | METHODS

2.1 | Patients

Twenty patients with PSP-RS, 21 patients with idiopathic PD, and 23 sex and age-matched healthy control subjects were consecutively recruited from those referred to the Movement Disorders Unit of the Institute of Neurology at the Magna Graecia University of Catanzaro, Italy between 2009 and 2017. Clinical diagnoses for all patients were established according to internationally diagnostic criteria and expert guidelines (Gelb, Oliver, & Gilman, 1999; Höglinger et al., 2017; Litvan et al., 1996) by one trained physician (M.M.) with more than 10 years of experience in movement disorders. Only patients meeting criteria for probable PSP (Litvan et al., 1996) were considered. These patients were then reclassified in PSP-RS according to new clinical diagnosis criteria of PSP (Höglinger et al., 2017). For each patient, a complete medical history with neurological examination and clinical assessment including the Unified Parkinson's Disease Rating Scale-Motor Examination (UPDRS-ME) (Fahn, Elton, & Unified Parkinson's Disease Rating Scale, 1987) and Hoehn and Yahr (H-Y) rating scale (Hoehn & Yahr, 1967) were performed.

2.2 | MRI acquisition

Neuroimaging data were acquired on a 3 Tesla Unit and using an 8-channels head coil (Discovery MR-750, General Electric, Milwaukee, WI). Head movements were minimized using foam pads around participants' heads. The protocol included: (1) a whole-brain T1-weighted scan (SPGR; Echo Time (ET) 3.7 ms, Repetition Time (TR) 9.2 ms, flip angle 12°, voxel-size 1.0 × 1.0 × 1.0 mm³); (2) a diffusion-weighted scan that was acquired using a spin-echo echo-planar imaging sequence (Echo Time (ET) 81 ms, Repetition Time (TR) 10,050 ms, band-width 250 KHz, matrix size 128 × 128; 80 axial slices, voxel size 2.0 × 2.0 × 2.0 mm³) with 27 isotropically distributed orientations for the diffusion-sensitizing gradients at a b-value of 1,000 s/mm², and (3) a fast Fluid-Attenuated Inversion-Recovery (FLAIR) axial sequence (Echo Time (ET) 100 ms, Repetition Time (TR) 9,500 ms, Inversion Time 2,250 ms, 36 axial slices, Refocus flip angle 90°, voxel size 0.5 × 0.5 × 4.0 mm³).

2.3 | Image processing: TDI construction

Pre-processing of diffusion data was performed as described previously (Pannek et al., 2011; Ziegler et al., 2014). Briefly, diffusion-weighted images were corrected for eddy current distortions using tools provided with FMRIB's Diffusion Toolbox (FDT, part of FMRIB Software Library FSL (Smith, Tournier, Calamante, & Connelly, 2013, <http://www.fmrib.ox.ac.uk/fsl>). Next, we used MRtrix (<http://www.mrtrix.org>) to estimate fiber orientation distributions using the constrained spherical deconvolution (CSD) method and modeling the response function by an axially symmetric tensor with an FA threshold of 0.7 in order to characterize the function in voxels with coherently oriented population of fibers (Tournier, Calamante, Gadian, &

Connelly, 2004). The number of spherical harmonic terms was set to 6 (Tournier, Calamante, & Connelly, 2007). Then, fiber tracking was performed employing the following tracking parameters: number of tracks = 10,000,000, FOD magnitude cutoff for terminating tracks = 0.1, minimum track length = 10 mm, maximum track length = 200 mm, minimum radius of curvature = 1 mm, tracking algorithm step size = 0.2 mm. Spherical-deconvolution Informed Filtering of Tractograms (SIFT) was also used to improve the quantitative nature of whole-brain streamlines reconstructions (number of tracks = 5,000,000) (Smith et al., 2013).

Next, fiber tracts were spatially normalized. In doing so, for every voxel the sum of the length of all streamlines passing through each voxel was calculated, giving a total pathlength map (TPM). Additionally, the number of streamlines traversing each voxel was recorded, rendering a track density image. The APM was then calculated dividing the TPM by the TDI. The APMs were then rigidly aligned to the MNI152 1 mm T1 template with mutual information and averaged to create an initial template. The APMs were then used to build a template through 4 iterations, beginning with an initial affine transformation followed by greedy symmetric diffeomorphic normalization (SyN) (Avants et al., 2010, 2011). For each subject, the transformations (rigid, affine, warp) were then individually inverted and applied in inverse order to a unit warp field generated in the final template space. Then, the tracks were normalized into template space with MRtrix, by warping each point along the fibers. This process ensured that the length of the streamlines was normalized together with the spatial location. Finally, track density images were generated from the normalized tracks, again with $1 \times 1 \times 1 \text{ mm}^3$ isotropic voxels. Normalization steps were performed using Advanced Normalization Tools (ANTS, <http://www.picsl.upenn.edu/ANTS/>). An optimal white matter mask was also generated from all TD images using the SPM8 Masking toolbox and the Luo–Nichols anti-mode method of automatic thresholding (Luo & Nichols, 2003; Ridgway et al., 2009).

2.4 | Statistical analysis

Whole-brain statistical analyses were performed using Randomize (5,000 iterations) (FSL). Differences in track density images between groups were assessed using a two-sample *t* test controlling for age and gender. Patients groups were first compared with each other, and then further compared with the healthy control population. Only

clusters with $p < .05$ after correcting for family-wise error rate were considered statistically significant. Moreover, Cohen's *d* was used to assess effect size for the group-wise comparisons (Cohen, 2013). Additional analyses were also conducted to assess associations between track density images and measures of disease severity and duration in PSP-RS and PD patients. Resulting *p*-value maps were transformed into MNI-152 space by applying an affine, 12-DOF transformation computed by registering the custom APM template to the MNI-152 template. In order to avoid creating false *p*-values, nearest neighbor interpolation was employed in this step.

We used the Pattern Recognition for Neuroimaging Toolbox (or PRoNT) (Schrouff et al., 2013) implemented in Matlab (<http://www.mnl.cs.ucl.ac.uk/pronto>) for pattern recognition. In particular, a binary support vector machine (SVM) approach was used to classify (a) patients with PSP-RS versus those with PD, (b) patients with PSP-RS versus control subjects, and (c) patients with PD versus control subjects using TDI as input images. In each of the analyses, leave one subject out cross-validation was performed. This means, that on each run, one subject was assigned to a testing set and the remaining subjects were assigned to a learning set. Then, the classification accuracy was expressed as a total performance on all runs. Voxel-wise discrimination map was also computed for each classification. This map shows the relative contribution of each voxel to the decision function with positive or negative weights to represent stronger representation for class one or two, respectively.

3 | RESULTS

3.1 | Behavioral data

Patients and control subjects had similar age and gender distributions. PSP-RS patients were more impaired than PD based on UPDRS, H-Y, and disease duration (Table 1).

3.2 | Voxelwise analysis of TDI

Statistically significant decreases in the number of streamlines in each voxel in PSP-RS patients, relative to PD patients, were found in brainstem, cerebellum, thalamic radiations, body of the corpus callosum, and corticospinal tract. Areas of decreased track density were strikingly symmetric between hemispheres (Figure 1). Moreover, Cohen's

TABLE 1 Demographic and clinical data of patients with PSP-RS, PD, and healthy controls

	PD group	PSP-RS group	HC group	<i>p</i> value
Participants	21	20	23	
Sex: No. of men/women	14/7	12/8	14/9	.89
Age at examination	70.47 ± 5.96	72.00 ± 5.96	70.54 ± 7.09	.69
Disease duration (years)	6.80 ± 5.09	3.10 ± 1.37	-	<.005
Age at onset (year)	65.00 ± 5.88	68.90 ± 5.87	-	.04
Hohen-Yahr score	2.04 ± 0.31	3.43 ± 0.78	-	<.001
UPDRS-ME	22.33 ± 7.68	39.40 ± 7.89	-	<.001

UPDRS-ME = Unified Idiopathic Parkinson's Disease Rating Scale; PD = Parkinson's Disease patients; PSP-RS = Progressive Supranuclear Palsy patients (Richardson's syndrome); HC = healthy controls.

All data are expressed as mean ± standard deviation. Chi-square test was used to test differences in gender distribution; one-way ANOVA was used to test differences in age; two sample *t*-tests were used for other variables.

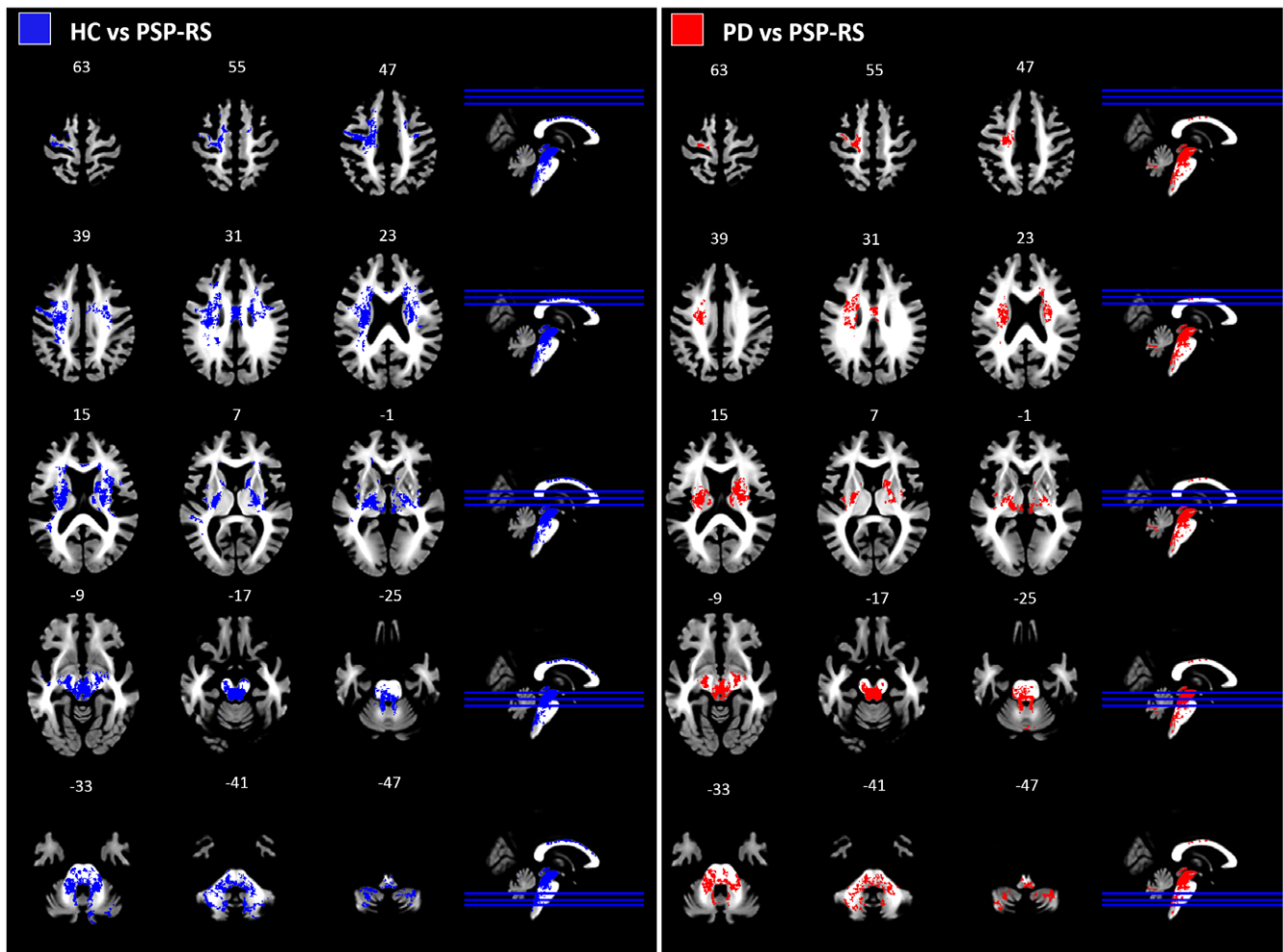


FIGURE 1 Overview of the decreases in track density. Left: Statistical map of decreased track density in PSP-RS patients relative to healthy controls; right: Statistical map of decreased track density in patients with PSP-RS relative to those with Parkinson disease. Clusters shown are significant at $p_{FWE} < 0.05$, estimated with threshold-free cluster enhancement. PD: Parkinson's disease patients; PSP-RS: Progressive Supranuclear palsy patients (Richardson's syndrome); HC: Healthy controls [Color figure can be viewed at wileyonlinelibrary.com]

d showed large effect size for each significant cluster ($d > 1.27$, see Supporting Information Materials for further details). Similar findings were obtained between PSP-RS patients and healthy controls ($d > 1.43$, see Supporting Information Materials for further details).

No statistically significant differences in TDI were observed between PD patients and healthy controls.

3.3 | Correlation with behavioral data

No significant correlation was found between track density values and clinical variables in both PSP and PD patients.

3.4 | Pattern recognition analysis

Considering patients groups, SVM based on whole brain analysis differentiated PD patients from PSP-RS patients with a sensitivity and specificity of 86 and 60%, respectively. The positive and negative predictive values (PPV/NPV) for the classifier were 80 and 69%, respectively. The area under the ROC curve (AUC) was 0.82. Similar results were obtained in the classification of PSP-RS patients and controls (Table 2). Regarding the voxel-wise discrimination map, Figure 2

shows the weighted-map of the global spatial patterns that best discriminate patients with PSP-RS from those with PD. The region showing the higher contribution to the decision function predictions was the superior cerebellar peduncles. This finding was confirmed by the improvement of the classification performance in distinguish PSP-RS and PD patients when restricting the analysis to the SCP. Indeed, we observed an AUC of 0.98, a sensitivity of 90% and a specificity of 100% in differentiating patients with PD from those with PSP-RS (Table 2, Figure 3). Similar improvements were observed in differentiating PSP-RS patients from healthy controls (Table 2).

3.5 | Discussion

In our study, we used track density imaging to study white matter alterations in patients with PSP-RS compared with those with PD and healthy controls. Our whole brain voxel-based analysis revealed a widespread pattern of fibers density changes in WM, potentially indicating alterations of brain microstructure and tissue integrity, in PSP-RS patients compared with PD patients. Specifically, significantly decrease in fibers density was observed in several tracts such as the corpus callosum, the arcuate fascicle, the superior longitudinal fascicle,

TABLE 2 Differentiation of patients with PSP from patients with PD using TDI

Classification analysis at whole-brain level					
	AUC	Specificity (%)	Sensitivity (%)	PPV (%)	NPV (%)
HC vs. PSP-RS	0.87	87	75	83	80
PD vs. PSP-RS	0.82	86	60	80	69
HC vs. PD	0.45	56	38	44	50
Classification analysis considering the superior cerebellar peduncles					
	AUC	Specificity (%)	Sensitivity (%)	PPV (%)	NPV (%)
HC vs. PSP-RS	1	100	95	100	96
PD vs. PSP-RS	0.98	100	90	100	91

AUC = area under the curve; PPV = positive predictive value; NPV = negative predictive value; PD = Parkinson's disease patients; PSP-RS = Progressive Supranuclear Palsy patients (Richardson's syndrome); HC = healthy controls.

In the upper side: Classification analysis was performed at whole-brain level; in the lower side: Classification analysis was performed using the voxels that belong to the superior cerebellar peduncle.

and CST bilaterally in PSP patients compared with PD and healthy controls. Abnormalities in density of WM streamlines also appeared to involve the midbrain, cerebellar peduncles, cerebellar WM, and thalamic radiations.

These findings are in agreement with post-mortem studies in PSP patients (Dickson, Ahmed, Algom, Tsuboi, & Josephs, 2010; Dickson et al., 2011; Ishizawa & Dickson, 2001; Schofield et al., 2011) and

confirm previous DTI studies demonstrating supra- and infratentorial WM changes in PSP (Cochrane & Ebmeier, 2013; Knake et al., 2010; Piattella et al., 2015).

In particular, the reduced fibers density found in the superior cerebellar peduncle confirms a strong involvement of this structure in PSP pathophysiology. This result is in line with previous DTI and morphometric MRI studies reporting significant diffusivity, volumetric.

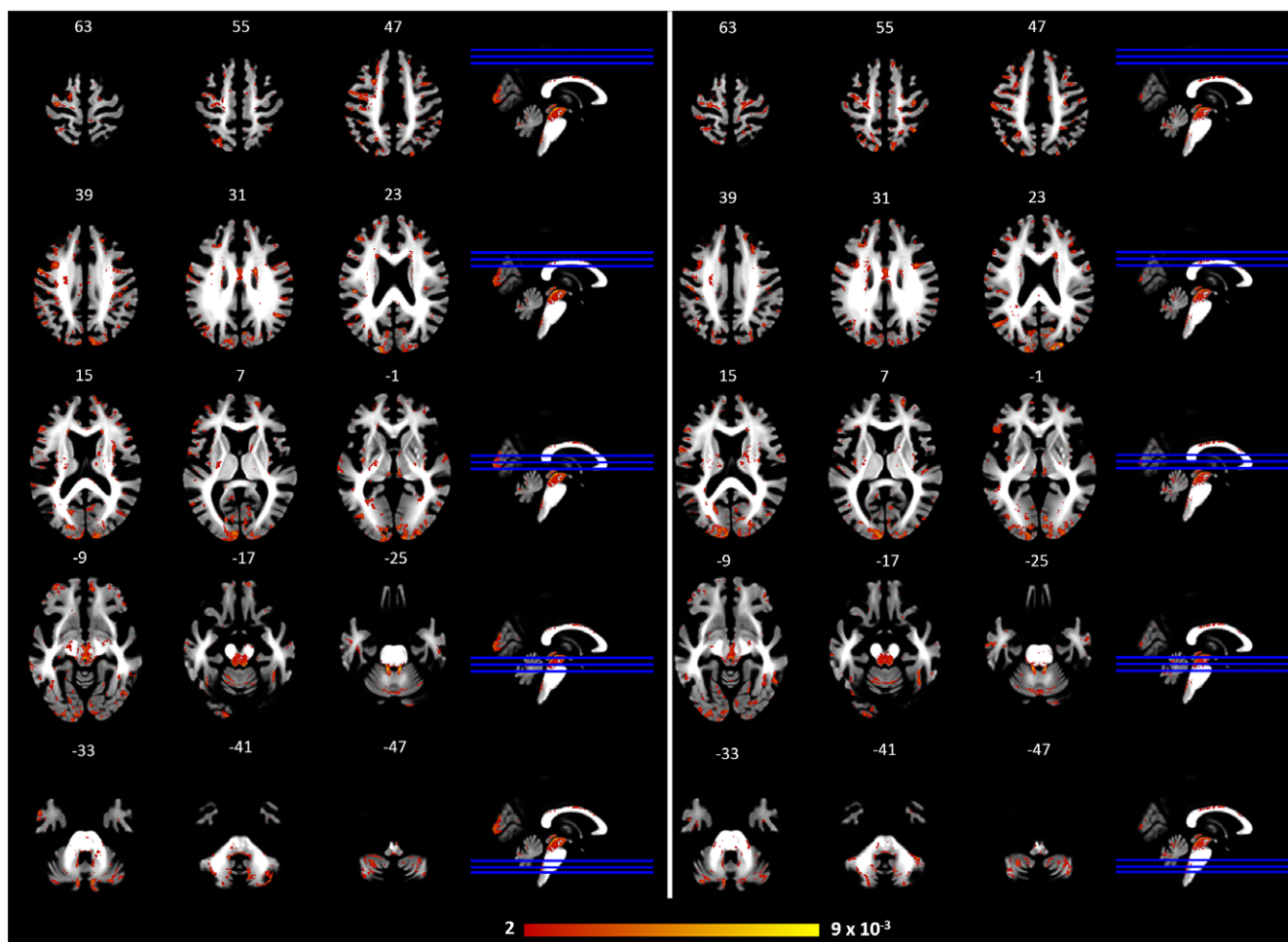


FIGURE 2 Left: weighted map of the global spatial patterns that show stronger representation for PSP-RS patients relative to HC; right: weighted map of the global spatial patterns that show stronger representation of PSP-RS patients relative to PD patients. PD: Parkinson's disease patients; PSP-RS: progressive supranuclear palsy patients (Richardson's syndrome); HC: Healthy controls [Color figure can be viewed at wileyonlinelibrary.com]

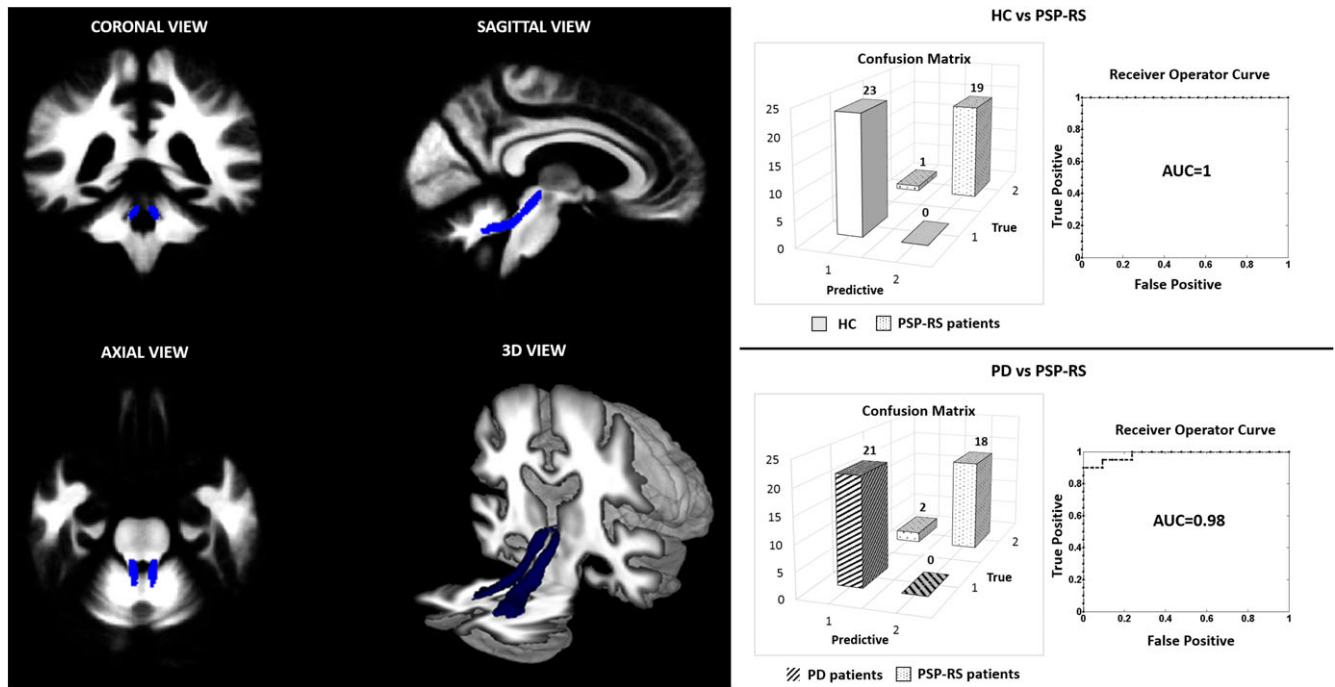


FIGURE 3 Performance of SVM classification in distinguishing patients with PSP-RS from those with PD and HC considering the voxels belonging to the superior cerebellar peduncle. AUC: area under the curve; PD: Parkinson's disease patients; PSP-RS: Progressive Supranuclear palsy patients (Richardson's syndrome); HC: healthy controls [Color figure can be viewed at wileyonlinelibrary.com]

and width changes of SCP in PSP-RS patients compared with those with PD and healthy controls (Blain et al., 2006; Knake et al., 2010; Nicoletti et al., 2008; Paviour, Price, Stevens, Lees, & Fox, 2005; Saini et al., 2012; Tsukamoto et al., 2012; Whitwell, Master, et al., 2011; Worker et al., 2014). Moreover, fibers density alterations in the SCP observed in our study correspond with pathological examination showing demyelination and high vulnerability of this region to tau accumulation in PSP (Tsuboi et al., 2003).

Relative to PD patients and healthy controls, PSP patients also showed decreased fibers density in thalamic radiations, midbrain, and dentate nucleus. These WM regions, together with the SCP, constitute the dentatorubrothalamic tract (DRTT). Specifically, the DRTT projects from the dentate nucleus of the cerebellum, through the SCP toward the red nucleus and then proceeds superiorly to the contralateral ventral lateral and anterior nuclei of the thalamus that serves as a relay station for projections to the cortex. This pathway is part of the functional "cerebrocerebellum circuit" and acts to coordinate the initiation, planning and timing of movement, but increasing evidence suggests an important role in cognitive function such as planning, verbal fluency, working memory, abstract thinking, and behavior (Middleton & Strick, 1998). The present findings provide new evidence that microstructural alterations of the DRTT play a crucial role in PSP pathophysiology. Moreover, our results further confirm previous pathological, DTI and resting-state functional MRI studies reporting significant degeneration and activated microglia, diffusivity changes and altered functional connectivity of the DRTT in PSP (Ishizawa & Dickson, 2001; Seki et al., 2018; Surova et al., 2015; Tsuboi et al., 2003; Whitwell, Avula, et al., 2011). Overall, these WM alterations may explain the functional motor deficit such as the

balance and posture deficits that characterize patients with PSP-RS (Paviour et al., 2005).

Of interest, we also noted reduced fibers density in the body of the corpus callosum and the cortical spinal tract of PSP patients compared with healthy controls and PD patients. These abnormalities, according with previous studies, may confirm cortical pathology reported in PSP population and the presence of pyramidal signs reported in about one-third of patients with PSP, respectively (Agosta et al., 2014; Ito et al., 2008; Litvan, 2004; Saini et al., 2012).

Finally, our study shows that track density imaging may offer promising markers to contribute to the diagnostic work-up of parkinsonian syndromes. In recent years, there has been increasing interest in using MRI-derived measures to classify parkinsonian disorders. Indeed, several studies explored the ability of morphometric and diffusion tensor imaging in distinguishing PSP patients from those with PD and healthy controls (Agosta et al., 2012, 2014; Bacchi, Chim, & Patel, 2018; Nicoletti et al., 2008; Nigro, Arabia, et al., 2017; Nigro, Morelli, et al., 2017; Quattrone et al., 2008; Seki et al., 2018; Seppi et al., 2003; Tsukamoto et al., 2012). More specifically, a recent DTI study observed a high accuracy in differentiating patients with PSP from those with PD using diffusion properties of SCP (AUC = 0.89) (Agosta et al., 2014). In our study, track density images of WM tracts showed a good performance in distinguishing PSP-RS patients from PD considering a whole brain voxel-based classification analysis. Of note, an AUC of 0.98 was observed in distinguishing PSP from PD when only the voxels belonging to the superior cerebellar peduncles were considered. This finding is not surprising since the SCP represents probably the tracts that showed the most significant alteration in diffusion properties in PSP-RS patients compared with PD patients and controls.

Taken together, these findings demonstrate the value of applying TDI approach to characterize WM changes in PSP-RS patients compared with PD patients and healthy controls. Although the TDI maps are generated from traditional DWI data, they can provide higher anatomical resolution than commonly used diffusion anisotropy maps. Moreover, the use of the CSD provides reliable fiber orientation estimations, even in voxels comprised of multiple fiber populations, generating more robust tracts reconstruction (Calamuneri et al., 2018). Of note, this study provide further evidence that CSD and TDI can be successfully applied using routine clinical MR protocols with low angular resolution and low b-value (Toselli et al., 2017). This finding, together with the possibility to implement the TDI procedure in a fully automatic way, suggests that TDI approach may help the clinicians to better understand microstructural WM involvement in several pathologic conditions.

This study is not without limitations. First, we examined a relatively small number of patients, and then our results have to be considered as preliminary to future studies on larger sample of patients. However, the large effect sizes reported in our group comparisons suggested that between-group differences in track density values were big enough to be reliably observed in our sample despite its small size. Second, our cases were not pathologically confirmed even if clinical evaluation was performed according the clinical criteria for diagnosing PSP, and was carried out by one of the authors with more than 10 years of experience in movement disorder especially in diagnosis and management of this disease. Third, we considered in our group of PSP only patients with Richardson's syndrome. So, further studies are needed to investigate the utility of the TDI to study the white matter alteration in others clinical phenotypes such as the PSP-parkinsonism. Moreover, patients in a very early stage of disease should be considered. Fourth, longitudinal studies are required to assess whether these abnormalities in structural brain network are predictive of the clinical-pathological evolution. Finally, it should be considered that even though the SVM approach showed high classification performance, the relatively small number of subjects might limit the generalization of our results. Moreover, a problem that might occur in pattern classification methods is the risk of overfitting the data due to the high-dimensionality of the data. Thus, further validations in independent and larger cohorts are necessary to confirm our results.

4 | CONCLUSIONS

In conclusion, we have shown that TDI is a useful approach for characterizing microstructure white matter alterations in PSP-RS patients compared with PD patients and healthy controls. Moreover, the presence of track density decrease in the superior cerebellar peduncle has shown to be a prominent feature of PSP-RS allowing a high sensitivity and specificity in the differentiation of patients with PSP-RS from those with PD.

ACKNOWLEDGMENTS

The authors are grateful to progressive supranuclear palsy patients, Parkinson's disease patients and controls who kindly participated in the experiment.

CONFLICT OF INTEREST

None of the authors has conflicted of interests.

ORCID

Salvatore Nigro  <https://orcid.org/0000-0001-7566-7983>

Aldo Quattrone  <https://orcid.org/0000-0003-2001-957X>

REFERENCES

- Agosta, F., Caso, F., Ječmenica-Lukić, M., Petrović, I. N., Valsasina, P., Meani, A., ... Filippi, M. (2018). Tracking brain damage in progressive supranuclear palsy: A longitudinal MRI study. *Journal of Neurology, Neurosurgery, and Psychiatry*, *89*, 696–701.
- Agosta, F., Galantucci, S., Svetel, M., Lukić, M. J., Copetti, M., Davidovic, K., ... Filippi, M. (2014). Clinical, cognitive, and behavioural correlates of white matter damage in progressive supranuclear palsy. *Journal of Neurology*, *261*, 913–924.
- Agosta, F., Pievani, M., Svetel, M., Ječmenica Lukić, M., Copetti, M., Tomić, A., ... Filippi, M. (2012). Diffusion tensor MRI contributes to differentiate Richardson's syndrome from PSP-parkinsonism. *Neurobiology of Aging*, *33*, 2817–2826.
- Attyé, A., Jean, C., Remond, P., Peyrin, C., Lecler, A., Boudiaf, N., ... Krainik, A. (2018). Track-weighted imaging for neuroretina: Evaluations in healthy volunteers and ischemic optic neuropathy. *Journal of Magnetic Resonance Imaging (JMIR)*, *48*, 737–747.
- Avants, B. B., Tustison, N. J., Song, G., Cook, P. A., Klein, A., & Gee, J. C. (2011). A reproducible evaluation of ANTs similarity metric performance in brain image registration. *NeuroImage*, *54*, 2033–2044.
- Avants, B. B., Yushkevich, P., Pluta, J., Minkoff, D., Korczykowski, M., Detre, J., & Gee, J. C. (2010). The optimal template effect in hippocampus studies of diseased populations. *NeuroImage*, *49*, 2457–2466.
- Bacchi, S., Chim, I., & Patel, S. (2018). Specificity and sensitivity of magnetic resonance imaging findings in the diagnosis of progressive supranuclear palsy. *Journal of Medical Imaging and Radiation Oncology*, *62*, 21–31.
- Blain, C. R. V., Barker, G. J., Jarosz, J. M., Coyle, N. A., Landau, S., Brown, R. G., ... Leigh, P. N. (2006). Measuring brain stem and cerebellar damage in parkinsonian syndromes using diffusion tensor MRI. *Neurology*, *67*, 2199–2205.
- Bozzali, M., Parker, G. J. M., Serra, L., Embleton, K., Gili, T., Perri, R., ... Cercignani, M. (2011). Anatomical connectivity mapping: A new tool to assess brain disconnection in Alzheimer's disease. *NeuroImage*, *54*, 2045–2051.
- Calamante, F. (2017). Track-weighted imaging methods: Extracting information from a streamlines tractogram. *MAGMA*, *30*, 317–335.
- Calamante, F., Tournier, J.-D., Jackson, G. D., & Connelly, A. (2010). Track-density imaging (TDI): Super-resolution white matter imaging using whole-brain track-density mapping. *NeuroImage*, *53*, 1233–1243.
- Calamante, F., Tournier, J.-D., Kurniawan, N. D., Yang, Z., Gyengesi, E., Galloway, G. J., ... Connelly, A. (2012). Super-resolution track-density imaging studies of mouse brain: Comparison to histology. *NeuroImage*, *59*, 286–296.
- Calamuneri, A., Arrigo, A., Mormina, E., Milardi, D., Cacciola, A., Chillemi, G., ... Quartarone, A. (2018). White matter tissue quantification at low b-values within constrained spherical Deconvolution framework. *Frontiers in Neurology*, *9*, 716.
- Canu, E., Agosta, F., Baglio, F., Galantucci, S., Nemni, R., & Filippi, M. (2011). Diffusion tensor magnetic resonance imaging tractography in progressive supranuclear palsy. *Movement Disorders*, *26*, 1752–1755.
- Cochrane, C. J., & Ebmeier, K. P. (2013). Diffusion tensor imaging in parkinsonian syndromes: A systematic review and meta-analysis. *Neurology*, *80*, 857–864.
- Cohen, J. (2013). *Statistical power analysis for the behavioral sciences* (2nd ed.). New York: Routledge.
- Dickson, D. W., Ahmed, Z., Algom, A. A., Tsuboi, Y., & Josephs, K. A. (2010). Neuropathology of variants of progressive supranuclear palsy. *Current Opinion in Neurology*, *23*, 394–400.

- Dickson, D. W., Hauw, J.-J., Agid, Y., & Litvan, I. (2011). Progressive supranuclear palsy and corticobasal degeneration. In D. W. Dickson & R. O. Weller (Eds.), *Neurodegeneration: The molecular pathology of dementia and movement disorders* (pp. 135–155). Oxford, UK: Wiley-Blackwell. <https://onlinelibrary.wiley.com/doi/abs/10.1002/9781444341256.ch15>
- Erbetta, A., Mandelli, M. L., Savoiardo, M., Grisoli, M., Bizzi, A., Soliveri, P., ... Girotti, F. (2009). Diffusion tensor imaging shows different topographic involvement of the thalamus in progressive supranuclear palsy and corticobasal degeneration. *AJNR. American Journal of Neuroradiology*, *30*, 1482–1487.
- Fahn, S., Elton, R., & Unified Parkinson's Disease Rating Scale (1987). In S. M. C. Fahn, M. Goldstein, & D. B. Calne (Eds.), *Recent developments in Parkinson's disease II* (pp. 153–163, 293–304). Florham Park, NJ: Macmillan Health Care Information.
- Gelb, D. J., Oliver, E., & Gilman, S. (1999). Diagnostic criteria for Parkinson disease. *Archives of Neurology*, *56*, 33–39.
- Hauw, J. J., Daniel, S. E., Dickson, D., Horoupian, D. S., Jellinger, K., Lantos, P. L., ... Litvan, I. (1994). Preliminary NINDS neuropathologic criteria for Steele-Richardson-Olszewski syndrome (progressive supranuclear palsy). *Neurology*, *44*, 2015–2019.
- Hoehn, M. M., & Yahr, M. D. (1967). Parkinsonism: Onset, progression and mortality. *Neurology*, *17*, 427–442.
- Höglinger, G. U., Respondek, G., Stamelou, M., Kurz, C., Josephs, K. A., Lang, A. E., ... Movement Disorder Society-endorsed PSP Study Group. (2017). Clinical diagnosis of progressive supranuclear palsy: The movement disorder society criteria. *Movement Disorders*, *32*, 853–864.
- Hughes, A. J., Daniel, S. E., Ben-Shlomo, Y., & Lees, A. J. (2002). The accuracy of diagnosis of parkinsonian syndromes in a specialist movement disorder service. *Brain*, *125*, 861–870.
- Ishizawa, K., & Dickson, D. W. (2001). Microglial activation parallels system degeneration in progressive supranuclear palsy and corticobasal degeneration. *Journal of Neuropathology and Experimental Neurology*, *60*, 647–657.
- Ito, S., Makino, T., Shirai, W., & Hattori, T. (2008). Diffusion tensor analysis of corpus callosum in progressive supranuclear palsy. *Neuroradiology*, *50*, 981–985.
- Knake, S., Belke, M., Menzler, K., Pilatus, U., Eggert, K. M., Oertel, W. H., ... Höglinger, G. U. (2010). In vivo demonstration of microstructural brain pathology in progressive supranuclear palsy: A DTI study using TBSS. *Movement Disorders*, *25*, 1232–1238.
- Litvan, I., Agid, Y., Calne, D., Campbell, G., Dubois, B., Duvoisin, R. C., ... Zee, D. S. (1996). Clinical research criteria for the diagnosis of progressive supranuclear palsy (Steele-Richardson-Olszewski syndrome): Report of the NINDS-SPSP international workshop. *Neurology*, *47*, 1–9.
- Litvan, I. (2004). Update on progressive supranuclear palsy. *Current Neurology and Neuroscience Reports*, *4*, 296–302.
- Luo, W.-L., & Nichols, T. E. (2003). Diagnosis and exploration of massively univariate neuroimaging models. *NeuroImage*, *19*, 1014–1032.
- Middleton, F. A., & Strick, P. L. (1998). Cerebellar output: Motor and cognitive channels. *Trends in Cognitive Sciences*, *2*, 348–354.
- Nicoletti, G., Lodi, R., Condino, F., Tonon, C., Fera, F., Malucelli, E., ... Quattrone, A. (2006). Apparent diffusion coefficient measurements of the middle cerebellar peduncle differentiate the Parkinson variant of MSA from Parkinson's disease and progressive supranuclear palsy. *Brain*, *129*, 2679–2687.
- Nicoletti, G., Rizzo, G., Barbagallo, G., Tonon, C., Condino, F., Manners, D., ... Quattrone, A. (2013). Diffusivity of cerebellar hemispheres enables discrimination of cerebellar or parkinsonian multiple system atrophy from progressive supranuclear palsy-Richardson syndrome and Parkinson disease. *Radiology*, *267*, 843–850.
- Nicoletti, G., Tonon, C., Lodi, R., Condino, F., Manners, D., Malucelli, E., ... Quattrone, A. (2008). Apparent diffusion coefficient of the superior cerebellar peduncle differentiates progressive supranuclear palsy from Parkinson's disease. *Movement Disorders*, *23*, 2370–2376.
- Nigro, S., Arabia, G., Antonini, A., Weis, L., Marcante, A., Tessitore, A., ... Quattrone, A. (2017). Magnetic resonance parkinsonism index: Diagnostic accuracy of a fully automated algorithm in comparison with the manual measurement in a large Italian multicentre study in patients with progressive supranuclear palsy. *European Radiology*, *27*, 2665–2675.
- Nigro, S., Morelli, M., Arabia, G., Nisticò, R., Novellino, F., Salsone, M., ... Quattrone, A. (2017). Magnetic resonance parkinsonism index and midbrain to pons ratio: Which index better distinguishes progressive supranuclear palsy patients with a low degree of diagnostic certainty from patients with Parkinson disease? *Parkinsonism & Related Disorders*, *41*, 31–36.
- Ohshita, T., Oka, M., Imon, Y., Yamaguchi, S., Mimori, Y., & Nakamura, S. (2000). Apparent diffusion coefficient measurements in progressive supranuclear palsy. *Neuroradiology*, *42*, 643–647.
- Osaki, Y., Ben-Shlomo, Y., Lees, A. J., Daniel, S. E., Colosimo, C., Wenning, G., & Quinn, N. (2004). Accuracy of clinical diagnosis of progressive supranuclear palsy. *Movement Disorders*, *19*, 181–189.
- Pannek, K., Mathias, J. L., Bigler, E. D., Brown, G., Taylor, J. D., & Rose, S. E. (2011). The average pathlength map: A diffusion MRI tractography-derived index for studying brain pathology. *NeuroImage*, *55*, 133–141.
- Paviour, D. C., Price, S. L., Stevens, J. M., Lees, A. J., & Fox, N. C. (2005). Quantitative MRI measurement of superior cerebellar peduncle in progressive supranuclear palsy. *Neurology*, *64*, 675–679.
- Piattella, M. C., Upadhyay, N., Bologna, M., Sbardella, E., Tona, F., Formica, A., ... Pantano, P. (2015). Neuroimaging evidence of gray and white matter damage and clinical correlates in progressive supranuclear palsy. *Journal of Neurology*, *262*, 1850–1888.
- Pierpaoli, C., & Basser, P. J. (1996). Toward a quantitative assessment of diffusion anisotropy. *Magnetic Resonance in Medicine*, *36*, 893–906.
- Prodoehli, J., Li, H., Planetta, P. J., Goetz, C. G., Shannon, K. M., Tangonan, R., ... Vaillancourt, D. E. (2013). Diffusion tensor imaging of Parkinson's disease, atypical parkinsonism, and essential tremor. *Movement Disorders*, *28*, 1816–1822.
- Quattrone, A., Nicoletti, G., Messina, D., Fera, F., Condino, F., Pugliese, P., ... Gallo, O. (2008). MR imaging index for differentiation of progressive supranuclear palsy from Parkinson disease and the Parkinson variant of multiple system atrophy. *Radiology*, *246*, 214–221.
- Ridgway, G. R., Omar, R., Ourselin, S., Hill, D. L. G., Warren, J. D., & Fox, N. C. (2009). Issues with threshold masking in voxel-based morphometry of atrophied brains. *NeuroImage*, *44*, 99–111.
- Saini, J., Bagepally, B. S., Sandhya, M., Pasha, S. A., Yadav, R., & Pal, P. K. (2012). In vivo evaluation of white matter pathology in patients of progressive supranuclear palsy using TBSS. *Neuroradiology*, *54*, 771–780.
- Schofield, E. C., Hodges, J. R., Macdonald, V., Cordato, N. J., Kril, J. J., & Halliday, G. M. (2011). Cortical atrophy differentiates Richardson's syndrome from the parkinsonian form of progressive supranuclear palsy. *Movement Disorders*, *26*, 256–263.
- Schrouff, J., Rosa, M. J., Rondina, J. M., Marquand, A. F., Chu, C., Ashburner, J., ... Mourão-Miranda, J. (2013). PRoNTTo: Pattern recognition for neuroimaging toolbox. *Neuroinformatics*, *11*, 319–337.
- Seki, M., Seppi, K., Mueller, C., Potrusil, T., Goebel, G., Reiter, E., ... Scherfler, C. (2018). Diagnostic potential of dentatorubrothalamic tract analysis in progressive supranuclear palsy. *Parkinsonism & Related Disorders*, *49*, 81–87.
- Seppi, K., Schocke, M. F. H., Esterhammer, R., Kremser, C., Brenneis, C., Mueller, J., ... Wenning, G. K. (2003). Diffusion-weighted imaging discriminates progressive supranuclear palsy from PD, but not from the parkinsonian variant of multiple system atrophy. *Neurology*, *60*, 922–927.
- Smith, R. E., Tournier, J.-D., Calamante, F., & Connelly, A. (2013). SIFT: Spherical-deconvolution informed filtering of tractograms. *NeuroImage*, *67*, 298–312.
- Surova, Y., Nilsson, M., Lätt, J., Lampinen, B., Lindberg, O., Hall, S., ... Hansson, O. (2015). Disease-specific structural changes in thalamus and dentatorubrothalamic tract in progressive supranuclear palsy. *Neuroradiology*, *57*, 1079–1091.
- Tessitore, A., Giordano, A., Caiazzo, G., Corbo, D., De Micco, R., Russo, A., ... Tedeschi, G. (2014). Clinical correlations of microstructural changes in progressive supranuclear palsy. *Neurobiology of Aging*, *35*, 2404–2410.
- Toselli, B., Tortora, D., Severino, M., Arnulfo, G., Canessa, A., Morana, G., ... Fato, M. M. (2017). Improvement in white matter tract reconstruction with constrained spherical deconvolution and track density mapping in low angular resolution data: A pediatric study and literature review. *Frontiers in Pediatrics*, *5*, 182.
- Tournier, J.-D., Calamante, F., & Connelly, A. (2007). Robust determination of the fibre orientation distribution in diffusion MRI: Non-negativity

- constrained super-resolved spherical deconvolution. *NeuroImage*, 35, 1459–1472.
- Tournier, J.-D., Calamante, F., Gadian, D. G., & Connelly, A. (2004). Direct estimation of the fiber orientation density function from diffusion-weighted MRI data using spherical deconvolution. *NeuroImage*, 23, 1176–1185.
- Tsuboi, Y., Slowinski, J., Josephs, K. A., Honer, W. G., Wszolek, Z. K., & Dickson, D. W. (2003). Atrophy of superior cerebellar peduncle in progressive supranuclear palsy. *Neurology*, 60, 1766–1769.
- Tsukamoto, K., Matsusue, E., Kanasaki, Y., Kakite, S., Fujii, S., Kaminou, T., & Ogawa, T. (2012). Significance of apparent diffusion coefficient measurement for the differential diagnosis of multiple system atrophy, progressive supranuclear palsy, and Parkinson's disease: Evaluation by 3.0-T MR imaging. *Neuroradiology*, 54, 947–955.
- Whitwell, J. L., Avula, R., Master, A., Vemuri, P., Senjem, M. L., Jones, D. T., ... Josephs, K. A. (2011). Disrupted thalamocortical connectivity in PSP: A resting-state fMRI, DTI, and VBM study. *Parkinsonism & Related Disorders*, 17, 599–605.
- Whitwell, J. L., Höglinger, G. U., Antonini, A., Bordelon, Y., Boxer, A. L., Colosimo, C., ... Movement Disorder Society-endorsed PSP Study Group. (2017). Radiological biomarkers for diagnosis in PSP: Where are we and where do we need to be? *Movement Disorders*, 32, 955–971.
- Whitwell, J. L., Master, A. V., Avula, R., Kantarci, K., Eggers, S. D., Edmonson, H. A., ... Josephs, K. A. (2011). Clinical correlates of white matter tract degeneration in progressive supranuclear palsy. *Archives of Neurology*, 68, 753–760.
- Wieshmann, U. C., Clark, C. A., Symms, M. R., Franconi, F., Barker, G. J., & Shorvon, S. D. (1999). Reduced anisotropy of water diffusion in structural cerebral abnormalities demonstrated with diffusion tensor imaging. *Magnetic Resonance Imaging*, 17, 1269–1274.
- Williams, D. R., de Silva, R., Paviour, D. C., Pittman, A., Watt, H. C., Kilford, L., ... Lees, A. J. (2005). Characteristics of two distinct clinical phenotypes in pathologically proven progressive supranuclear palsy: Richardson's syndrome and PSP-parkinsonism. *Brain*, 128, 1247–1258.
- Worker, A., Blain, C., Jarosz, J., Chaudhuri, K. R., Barker, G. J., Williams, S. C. R., ... Simmons, A. (2014). Diffusion tensor imaging of Parkinson's disease, multiple system atrophy and progressive supranuclear palsy: A tract-based spatial statistics study. *PLoS One*, 9, e112638.
- Ziegler, E., Rouillard, M., André, E., Coolen, T., Stender, J., Balteau, E., ... Garraux, G. (2014). Mapping track density changes in nigrostriatal and extranigral pathways in Parkinson's disease. *NeuroImage*, 99, 498–508.

SUPPORTING INFORMATION

Additional supporting information may be found online in the Supporting Information section at the end of the article.

How to cite this article: Nigro S, Bianco MG, Arabia G, et al. Track density imaging in progressive supranuclear palsy: A pilot study. *Hum Brain Mapp*. 2019;40:1729–1737. <https://doi.org/10.1002/hbm.24484>